

# Pathways of soil genesis in the Coast Range of Oregon, USA

Katherine S. Lindeburg · Peter Almond ·  
Josh J. Roering · Oliver A. Chadwick

Received: 16 August 2012 / Accepted: 10 December 2012 / Published online: 9 January 2013  
© Springer Science+Business Media Dordrecht 2013

## Abstract

**Background and Aims** Soil chronosequences on marine terraces along the Pacific Coast of California and Oregon show evidence of podzolization, though soils ultimately evolve to Ultisols. It is not clear if this pathway of soil evolution can be extended to the humid, inland Oregon Coast Range.

**Methods** We analyzed soil properties for a fluvial terrace chronosequence sampled along the Siuslaw River (Oregon, USA) about 50 km from the Pacific coast. The seven terraces ranged in age from <3.5 ky to nearly 1,000 ky.

**Results** There was no evidence of early podsolization. Instead, evidence was found that andisolization starts early and occurs even in older soils when pedogenic iron accumulation and clay synthesis and illuviation dominate. Soils develop the morphology characteristic

of Ultisols sometime between 20 and 70 ky, but high levels of oxalate extractable iron and aluminum satisfy criteria of an andic subgroup. Alfisols are not formed as an intermediary stage.

**Conclusions** The lack of Spodosols inland is due to the inland shift from udic to ustic or xeric moisture regime, which favors summer drying and ripening of short-range order minerals rather than deep leaching or translocation. Other factors are higher pH, different organic chemistry and faster calcium cycling under the Douglas fir inland when compared to the Sitka spruce of the coastal terraces.

**Keywords** Chronosequence · Fluvial terraces · Oregon Coast Range · Podzolization · Ultisols

## Introduction

Marine or fluvial terraces form episodically over long time scales and allow us to sample soil chronosequences to infer surficial processes (McFadden and Knuepfer 1990; Bull 1991; Barrett and Schaetzl 1992; Singer et al. 1992; Muhs 1982; Jenny et al. 1969). Much of what we know about soil development comes from these studies (Bockheim 1980; Schaetzl et al. 1994; Birkeland 1999), but it is unclear how relevant the resulting conceptual or quantitative models are to regional landscapes or even if chronosequences on different types of landforms will yield the same models.

Marine terraces along the Oregon coast preserve records of eustatic high sea level stands and tectonic uplift. They comprise relict strath-like platforms that extend inland from the coast and carry a surficial deposit of sand derived from the paleobeach with

---

Responsible Editor: Leo M. Condron.

---

K. S. Lindeburg · O. A. Chadwick (✉)  
Department of Geography, University of California,  
Santa Barbara, CA, USA  
e-mail: oac@geog.ucsb.edu

K. S. Lindeburg  
e-mail: klindeburg@gmail.com

P. Almond (✉)  
Department of Soil and Physical Sciences, Lincoln University,  
Christchurch, New Zealand  
e-mail: peter.almond@lincoln.ac.nz

J. J. Roering  
Department of Geological Sciences, University of Oregon,  
Eugene, OR, USA  
e-mail: jroering@uoregon.edu

subsequent additions of reworked, wind-blown beach sand (Kelsey et al. 1996; Kelsey 1990). These terraces have been studied to understand soil genesis in the Pacific Northwest. Nettleton et al. (1982), Bockheim et al. (1992; 1996) and Langley-Turnbaugh and Bockheim (1997) demonstrated that in-situ clay formation and podzolization dominate early pedogenesis leading to development of Inceptisols and Spodosols; over longer time periods, podzolization and argilluviation act concurrently to form spodic horizons overlying argillic horizons in soils that classify as Spodosols; whereas in late stages of soil development, argilluviation and 1:1 silicate clay neof ormation dominate and Ultisols form as a result. The coarse temporal resolution provided by the marine terraces notwithstanding, this model provides a valuable framework for understanding pedogenesis along the Pacific coast and in marine terrace cover sediments, but its applicability to soils further inland has not been tested. For instance, it is not clear what role local factors, such as proximity to salt-rich sea-spray and wind-blown beach sands, or the moderating influence of coastal temperatures, would exert on soil development, either directly by altering chemical and physical pathways or indirectly by determining vegetation communities and/or rates of bioturbation.

We present data from a fluvial terrace chronosequence in the Oregon Coast Range to test the coastal model of pedogenesis. The fluvial terraces are situated about 50 km inland, and their soils formed in mineralogically comparable sediments as the cover sands on the marine terraces. The purposes of this paper are to: (1) present detailed soil chemical, physical, and mineralogical analyses of the fluvial terrace chronosequence; (2) relate soil properties to time-dependent soil-forming processes; (3) compare them to the Bockheim model; and (4) identify possible causes for differences between the fluvial and marine terrace chronosequences and hence differences in soil genesis pathways.

## Methods and materials

### Setting

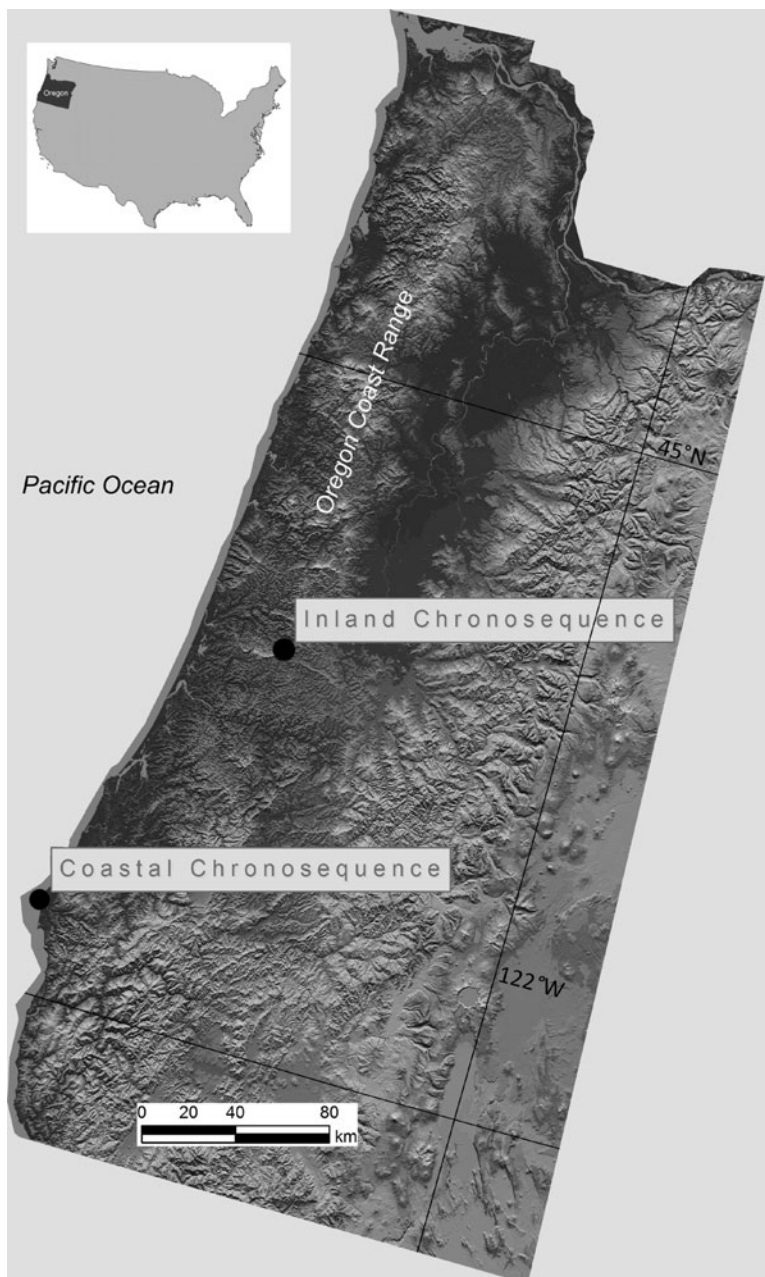
Seven soils were sampled from sequential fluvial terraces located on the western edge of a meander along the Siuslaw River within the Oregon Coast Range (Fig. 1). The terraces are designated as T1 (the lowest in elevation and youngest) through T7 (the highest in

elevation and oldest) (Table 1). The local geologic uplift rate, as measured from dating of nearby marine terraces, is  $<0.1$  to  $0.3 \text{ mm}\cdot\text{yr}^{-1}$  (Kelsey et al. 1996) and results from the continued convergence of the Juan de Fuca Plate with the North American Plate (Orr et al. 1992). The Oregon Coast Range has an average denudation rate of  $0.05$  to  $0.3 \text{ mm}\cdot\text{yr}^{-1}$  (Reneau and Dietrich 1991; Bierman et al. 2001; Heimsath et al. 2001), roughly balancing the uplift rate and suggesting a topographic steady-state over millennial timescales (Reneau and Dietrich 1991; Roering et al. 1999; Montgomery 2001). The ages of the two youngest terraces (Terraces 1 and 2) were determined by radiocarbon dating of detrital charcoal collected from soil pits. Ages of the five other terraces were calculated from elevation above modern river valley and incision rate (further details on dating methods can be found in Almond et al. 2007).

The terraces straths where visible are cut in the Tye Formation, which is a lithified Eocene-aged sandstone-dominated ramp turbidite sequence, derived from the Idaho batholith to the east and proximal metamorphic and volcanic features associated with the proto-Cascade Range (Heller et al. 1985). The Tye Formation is geologically described as being an arkosic, lithic, and feldspathic wacke, and to a lesser degree, as a volcanic wacke. The mineralogy of these rocks consists of quartz, andesine and calcic andesine, and lithic fragments. Lesser mineral constituents include potassium feldspars, smectite, calcite, and micas (Snively et al. 1964; Heller and Dickinson 1985; Ryu 2003). Sandy alluvial coverbeds over the straths are obvious on Terraces 1 and 2, but these become indistinguishable from the underlying weathered Tye on older terraces.

The fluvial terrace study area experiences warm summers with light rains and wet and cool fall and winter months (Patching 1987). Winds from the Pacific Ocean have a moderating effect on the climate as they reach the inland fluvial terraces by being funneled through narrow river gorges. Freezing temperatures and snow are common in the winter. It is likely that near-surface horizons may be affected by freeze-thaw cycles. Mean annual average temperature (MAAT) of the study area is  $10$ – $11.1$  °C, and mean annual precipitation (MAP) is  $1,800$ – $2,600$  mm (Table 1). Due to elevation differences of the terraces, MAAT and MAP may vary among the sampling sites, although all terrace soils have mesic temperature.

**Fig. 1** Location of fluvial terrace chronosequence relative to coastal terrace chronosequences in the Cape Arago and Cape Blanco regions studied by (Bockheim et al. 1992; Bockheim et al. 1996; Langley-Turnbaugh and Bockheim 1997; Langley-Turnbaugh and Bockheim 1998)



Patching (1987) infers an udic moisture regime for soil series mapped in the area but the 2-min grid cell Soil Moisture Regimes Map (NRCS 2003) places the site on the boundary of ustic and xeric soil moisture regimes.

The terraces support Douglas fir [*Pseudotsuga menziesii* (Mirbel) Franco] as the dominant tree species and Western hemlock [*Tsuga heterophylla* (Raf.) Sarg.] as a subdominant species. Less abundant species include Sitka spruce [*Picea sitchensis* (Bong.)

Carr.] and Western red cedar [*Thuja plicata* (Donn) ex D. Don]. Understory species include salal (*Gaultheria shallon* Pursh), salmon berry (*Rubus spectabilis* Pursh) and evergreen huckleberry (*Vaccinium ovatum* Pursh) (Patching 1987).

#### Field sampling and laboratory analyses

The first five fluvial terraces have planar morphology. Soil sampling locations were selected to represent

**Table 1** Site characteristics

| Terrace | Terrace age (ky) | Elevation (m) <sup>c</sup> | Depth of weathering (cm) <sup>d</sup> | MAP (mm) <sup>e</sup> | MAAT (°C) <sup>e</sup> |
|---------|------------------|----------------------------|---------------------------------------|-----------------------|------------------------|
| T1      | 3.5 <sup>a</sup> | 85.5                       | 20                                    | 1,800                 | 10.5                   |
| T2      | 20 <sup>a</sup>  | 89.0                       | 109                                   | 1,900                 | 11                     |
| T3      | 69 <sup>b</sup>  | 94.3                       | 260                                   | 1,900                 | 11                     |
| T4      | 140 <sup>b</sup> | 106.9                      | 310                                   | 2,400                 | 11                     |
| T5      | 200 <sup>b</sup> | 117.6                      | 460                                   | 2,400                 | 11                     |
| T6      | 908 <sup>b</sup> | 248.9                      | >910                                  | 2,550                 | 9.5                    |
| T7      | 990 <sup>b</sup> | 263.8                      | >1,100                                | 2,550                 | 9.5                    |

<sup>a</sup>From Almond et al. 2007, based on radiocarbon of detrital charcoal;

<sup>b</sup>from Almond et al. 2007, using uplift rates and terrace elevation;

<sup>c</sup>from Almond et al. 2007, using GPS during fieldwork;

<sup>d</sup>from Almond et al. 2007, equivalent to base of saprolite;

<sup>e</sup>from Soil Survey of Lane County Area, Patching, W.R., 1987

modal conditions as interpreted from a series of auger holes (à la Barrett and Schaetzl 1993). The two oldest sites are represented by remnants of eroded and dissected terraces and exhibit evidence of minor surface erosion. These terraces were sampled from logging road-cut exposures and augmented by auger holes to sample deeper weathering zones. Soil pits were dug to at least 1.4 m in the first five terraces. Soils were described by horizon using the methods of Milne et al. (1995) and sampled in 10 cm increments. Bulk density was measured using a core of known bulk volume.

Soil samples were dried for 48 h at 105 °C. Base cations were determined by extracting soil with pH 7 1 M NH<sub>4</sub>OAc and analyzed by flame atomic absorption spectrometry. Cation exchange capacity (CEC) was determined after sequentially leaching soil with 1 M NH<sub>4</sub>OAc buffered at pH 7 and 1 M KCl. NH<sub>4</sub> was analyzed on a colorimetric auto-analyzer. Electrical conductivity (mS/cm) and pH were measured on 2:1 water to soil solution with bench-top meters. Particle size distribution was determined by the pipette method after removal of organic matter using H<sub>2</sub>O<sub>2</sub> and iron oxides using dithionite-citrate-bicarbonate (Jackson 1954). Sand fractions were separated by wet sieving and saved for mineralogical analyses. Minerals in the fine-sand fraction (0.125 mm–0.053 mm) were identified by X-ray diffraction on a Bruker D8 Advance Diffractometer with a CuK beam. Randomly-mounted and untreated samples were scanned between

4° and 60° of 2θ with a step size of 0.015° and step time of 0.5 s. Software and a powder diffraction file database were used to process diffractograms and to identify minerals, with the requirement of identifying at least three diagnostic peaks to determine the proportion of quartz, potassium feldspar, and plagioclase feldspars (Moore and Reynolds 1997).

Metals were extracted with 0.1 M sodium pyrophosphate (McKeague 1967), 0.2 M ammonium acid oxalic acid buffered at pH 3 (McKeague and Day 1966), and dithionite-citrate-bicarbonate (Mehra and Jackson 1960). Extracts were analyzed for Fe and Al by atomic absorption spectroscopy. Concentrations of C and N were determined using a Carla-Erba analyzer after samples were ground to a fine mesh.

Analyses were conducted on 10-cm sampling depth increments, rather than on channel samples representing entire horizons. For horizons with multiple 10-cm sample increments, all 10-cm values within a horizon were used for calculations associated with classification and then depth-weighted, averaged and reported as single values associated with the horizon from which they were sampled. Analytical precision was checked against standard reference samples. For XRD, we prepared multiple slides for a select number of samples. Laboratory analyses were run on duplicates. Replication of particle size distribution, CEC, pedogenic oxides, organic C, and pH resulted in ranges of variation <6 %. Replication of base cations and organic N resulted in ranges of variation <20 % which likely was due to enhanced error when measuring near detection.

Profile mass contents ( $m_p$ ) of select constituents (e.g., pedogenic oxides, organic carbon, clay content) were calculated as:

$$m_p = \sum_{n=1}^{n=k} \rho_s \cdot z_w \cdot C_j \quad (1)$$

where  $\rho_s$  is bulk density of soil in g·cm<sup>3</sup>,  $z_w$  is horizon thickness in cm,  $C_j$  is concentration, and  $k$  is number of soil horizons. In addition to depth of solum, mass contents of select pedogenic properties were summed to depths of 0.4 m and 1.0 m in order to enable mass-area comparisons of soil profiles with varying thicknesses.

Hurst's Redness Rating (RR) was calculated as (Hurst, 1977):

$$RR = H \cdot V \cdot C^{-1} \quad (2)$$

where  $H$  is hue,  $V$  is soil value, and  $C$  is soil chroma on moist field samples. Munsell hues for Hurst's Redness Rating were converted from 5R to 5, 10R to 10, 5YR to 15, and 10YR to 20. In this method of quantifying soil color, soil redness and RR are inversely related—the redder the soil, the lower the RR value.

## Results

### Morphological and physical properties

The Terrace 1 (T1) pedon consists of multiple packets of stream sediments and buried soils. The uppermost packet of stream sediments is about 35 cm thick and was probably deposited by a flood in 1964. It is composed of coarse sand with <5 % clay and <7 % silt, with field moist colors of 10YR 4/2 to 10YR 5/3 (Table 2). The first buried soil (40–107 cm) has a sandy loam texture throughout with 10YR 3/1 to 10YR 4/6 colors. Soil textures on all other terraces are loam, sandy clay loam, clay loam, and clay, with a dominant particle size class of silt on T2 and clay on all other terraces. Silt contents are generally higher in surface horizons and some shallow B horizons than in the deeper B and BC horizons, which is likely due to eolian inputs to the surface. Soils on all terraces except the youngest have subsurface zones of clay accumulation that thicken with increasing age. The profile maximum clay percentage increases with terrace age and ranges from about 35 % (T2) to 75 % (T6), and clay content integrated to 1 m increases from 295 (T2) to 732 kg·m<sup>-2</sup> (T6) (Fig. 2a). Soil colors get redder with age, reaching hues of 10R in the oldest terraces.

Sand mineralogy of the terrace soils is dominated by quartz (Table 2). Less abundant and more variable minerals in the fine sand particle size class include plagioclase and potassium feldspars. Feldspar (sum of plagioclase and potassium feldspars) to quartz ratio (F/Q) indicates large depth variation in the relative abundance of weatherable minerals on individual terraces and across the chronosequence (Table 2). With increasing terrace age there is a strong decline in total feldspars relative to quartz (F/Q) and a decrease in the plagioclase to potassium feldspar (P/K) ratio (Fig. 2b).

### Exchange properties, organic carbon, and pH

Soils on all terraces are acidic, depleted in base cations, and have moderate cation exchange capacities

(CEC) (Table 3). With the exception of T1, exchangeable base cation concentrations generally follow the pattern of Ca>K≈Mg>Na. Exchangeable Ca (xCa), Mg (xMg), and K (xK) are highest in the upper 20 cm and decrease with depth to the base of solum. The decrease in xCa in uppermost horizons to deeper horizons is abrupt, whereas the decrease in xMg and xK with depth is gradual. The concentration of total base cations is highest in the uppermost ~50 cm (1.1 to 5.3 cmolc·kg<sup>-1</sup>) and decreases with depth. The solum depth-weighted average concentration of total base cations decreases rapidly from 4.6 (T1) to 0.75 (T3) cmolc·kg<sup>-1</sup> and remains relatively constant after that (Fig. 2c). Percent base saturation drops from a depth-weighted solum average of 35 % in T1 to 3.6 % in T2 and remains low throughout the rest of the chronosequence (Fig. 2c). Cation exchange capacity in the terrace soils is maximum in A horizons and generally decreases with depth (Fig. 3b). Maximum B horizon CEC across the chronosequence is highest in the T2 pedon (39 cmolc·kg<sup>-1</sup>) (Fig. 2c). Terraces older than T2 have lower maximum B horizon CEC values (~20 cmolc·kg<sup>-1</sup> in T3–T7) with no clear age-dependent trend (Fig. 2b). Soil acidity is lowest in the youngest soil and ranges from moderately acidic to strongly acidic (pH=5.7–5.4). All other soils are strongly or very strongly acidic (pH=4.6–5.4) and vary little with depth (0.1–0.3 pH units).

The concentration of organic carbon in all profiles is highest in the surface horizons (ranging from 2 to 9 %) and decreases abruptly with depth (Table 3; Fig. 3a). Within the intermediate and old terrace soil profiles, depth where organic carbon concentration decreases to <1.0 % coincides with depth of profile maximum clay content and/or the upper boundary of clay accumulation zones (~40–70 cm). With the exception of the buried soils in T1, terrace soils have no subsurface maxima in organic carbon concentrations that would suggest the existence of Bh horizons. Depth-integrated carbon values do not show strong time-dependent patterns (Fig. 2d).

### Extractable Al, Fe, and Si

The surface soil on T1 lacks an accumulation of pedogenic Fe and Al. This is consistent with other field and lab data that reflect little pedogenic development (Table 4). The irregular depth distribution of metal oxides corresponds to horizons with somewhat greater

**Table 2** Selected physical and mineralogical data for fluvial terrace pedons

| Terrace | Horizon | Horizon depth (cm) | Color     | Bulk density (g·cm <sup>-3</sup> ) | Particle size distribution |          |          | Fine sand mineralogy <sup>a</sup> |     |
|---------|---------|--------------------|-----------|------------------------------------|----------------------------|----------|----------|-----------------------------------|-----|
|         |         |                    |           |                                    | Sand (%)                   | Silt (%) | Clay (%) | P/K                               | F/Q |
| 1       | A       | 0–10               | 10YR 3/2  | 0.91                               | 89.4                       | 6.1      | 4.5      | 3.1                               | 0.5 |
|         | C1      | 10–25              | 10YR 4/3  | 1.28                               | 91.9                       | 5.8      | 2.3      | 2.3                               | 0.6 |
|         | C2      | 25–35              | 10YR 5/3  | 1.14                               | 90.4                       | 6.0      | 3.6      | 3.6                               | 0.6 |
| 2       | A       | 0–7                | 10YR 3/2  | 0.63                               | 30.7                       | 42.0     | 27.2     |                                   |     |
|         | Bw1     | 7–38               | 10YR 4/2  | 0.93                               | 30.3                       | 45.3     | 24.4     | 0.4                               | 1.0 |
|         | Bw2     | 38–88              | 10YR 3/3  | 1.02                               | 25.9                       | 41.6     | 32.5     | 1.9                               | 0.1 |
|         | BC      | 88–109             | 2.5YR 5/4 | 1.15                               | 24.4                       | 41.2     | 34.5     |                                   |     |
|         | C1      | 109–122            | 2.5Y 6/4  | 1.29                               | 34.5                       | 36.5     | 29.0     |                                   |     |
| 3       | A       | 0–28               | 10YR 4/2  | 1.02                               | 39.0                       | 33.9     | 27.1     | 1.1                               | 0.5 |
|         | Bt1     | 28–44              | 10YR 4/3  | 1.25                               | 32.0                       | 29.2     | 38.7     |                                   |     |
|         | Bt2     | 44–68              | 7.5YR 4/4 | 1.12                               | 31.5                       | 26.2     | 42.3     | 5.3                               | 0.1 |
|         | Bt3     | 68–113             | 5YR 4/4   | 1.19                               | 30.0                       | 25.9     | 44.1     | 0.3                               | 0.1 |
|         | BCt1    | 113–200            | 7.5YR 4/4 | 1.32                               | 34.6                       | 24.8     | 40.5     | 0.0                               | 0.1 |
|         | BC2     | 200–245            | 10YR 5/8  | 1.47                               | 61.8                       | 21.6     | 16.6     | 1.4                               | 0.2 |
| 4       | A       | 0–28               | 7.5YR 3/2 | 1.00                               | 30.4                       | 32.9     | 36.7     | 0.9                               | 0.2 |
|         | Bw      | 28–42              | 5YR 4/3   | 1.00                               | 31.1                       | 31.6     | 37.3     |                                   |     |
|         | Bt      | 42–75              | 5YR 4/6   | 1.04                               | 30.0                       | 26.7     | 43.3     |                                   |     |
|         | 2Bt2    | 75–120             | 5YR 4/4   | 1.31                               | 29.6                       | 26.5     | 43.9     |                                   |     |
|         | 2Bw1    | 120–190            | 7.5YR 5/6 | 1.19                               | 34.3                       | 29.3     | 36.5     | 1.2                               | 0.0 |
|         | 2Bw2    | 190–240            | 7.5YR 4/6 | 1.36                               | 37.8                       | 34.2     | 28.1     | 1.7                               | 0.1 |
| 5       | A       | 0–21               | 5YR 3/2   | 0.81                               | 20.0                       | 38.8     | 41.2     | 0.0                               | 0.0 |
|         | Bw      | 21–50              | 5YR 4/4   | 1.04                               | 18.8                       | 38.6     | 42.7     | 0.4                               | 0.1 |
|         | Bt1     | 50–100             | 2.5YR 3/6 | 1.21                               | 19.1                       | 24.8     | 56.1     |                                   |     |
|         | Bt2     | 100–170            | 2.5YR 4/6 | 1.24                               | 25.2                       | 28.9     | 45.7     | 2.6                               | 0.1 |
| 6       | AB      | 8–39               | 2.5YR 4/4 | 1.10                               | 15.4                       | 22.2     | 62.3     | 0.5                               | 0.0 |
|         | Bt1     | 39–92              | 10R 4/6   | 1.04                               | 10.7                       | 14.8     | 74.5     | 2.0                               | 0.0 |
|         | Bt2     | 92–192             | 2.5YR 3/6 | 1.03                               | 13.6                       | 18.9     | 67.5     | 0.3                               | 0.0 |
|         | Bt3     | 192–232            | 2.5YR 4/8 | 1.42                               | 18.2                       | 34.2     | 47.6     |                                   |     |
| 7       | A       | 0–20               | 5YR 3/4   | 0.77                               | 21.9                       | 31.2     | 46.8     | 0.9                               | 0.0 |
|         | Bw      | 20–37              | 2.5YR 3/4 | 1.04                               | 18.4                       | 30.4     | 51.2     | 0.1                               | 0.0 |
|         | Bt1     | 37–73              | 2.5YR 3/6 | 0.96                               | 13.0                       | 19.2     | 67.8     |                                   |     |
|         | 2Bt1    | 73–140             | 10R 4/6   | 1.19                               | 14.2                       | 20.1     | 65.6     |                                   |     |

Blanks indicate unanalyzed sample

<sup>a</sup> Mineralogy based on relative intensities of diagnostic peaks of quartz (Q), plagioclase feldspars (P), and potassium feldspar (K). P/K is ratio of plagioclase feldspars to potassium feldspar; F/Q is ratio of total feldspars (sum of plagioclase and potassium feldspars) to quartz

development, as suggested by small but observable increases in soil structure, darker and redder colors, and measureable increases in organic carbon and percent clay (Table 4; not all data shown). Soils on T2 through T7 have profile depth trends for oxalate extractable Al (Alo) and pyrophosphate extractable Al (Alp) that show maxima in A horizons and a decline

with depth (Table 4; Fig. 3c). Oxalate extractable Fe (Feo) and Na pyrophosphate extractable Fe (Fep) have depth trends similar to those of Alo and Alp, although percentages of oxalate and pyrophosphate extractable Al are consistently higher than those of Fe (Fig. 3d). Further distinction between the extractable components of Fe and Al are observed in the depth at which

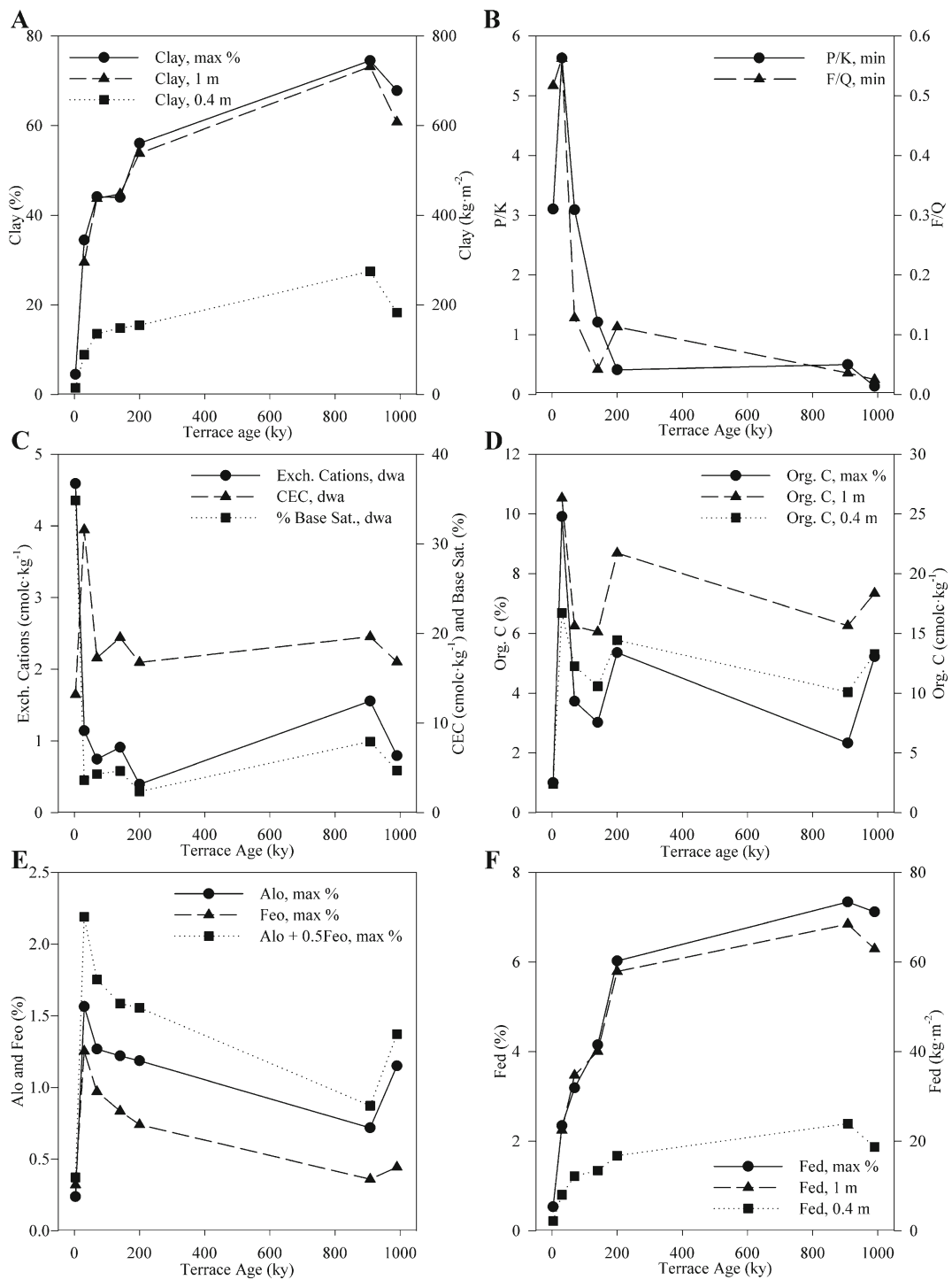


**Fig. 2** Physical, chemical, and mineralogical age-trends. Panels (a) and (d) through (f) show solum maxima (black circle) and mass per area to 1.0 m (black up-pointing triangle) and 0.4 m (black small square). Chemical properties in (c) are depth-weighted to solum base. Fine sand mineralogy in (b) is profile-maxima of the ratio of plagioclase feldspars to potassium feldspar (P/K) and

profile-minima of the ratio of total feldspars (sum of plagioclase and potassium feldspars) to quartz (F/Q). Clay (a) and Fed (f) both increase rapidly from low values in the youngest terrace to nearly maximum values in T5. Fine sand mineralogy (b) becomes enriched in quartz at the expense of feldspars; plagioclase feldspars declines with terrace age faster than potassium feldspar

**Table 3** Chemical properties for selected horizons

| Terrace | Horizon | Horizon depth (cm) | Organic C (%) | pH  | Exchangeable cations          |      |      |      | CEC  |
|---------|---------|--------------------|---------------|-----|-------------------------------|------|------|------|------|
|         |         |                    |               |     | xCa                           | xMg  | xNa  | xK   |      |
|         |         |                    |               |     | (cmolc·kgsoil <sup>-1</sup> ) |      |      |      |      |
| 1       | A       | 0–10               | 1.00          | 5.4 | 3.40                          | 0.21 | 0.21 | 1.50 | 11.5 |
|         | C1      | 10–25              | 0.33          | 5.5 | 2.47                          | 0.45 | 0.24 | 0.85 | 11.9 |
|         | C2      | 25–35              | 0.50          | 5.7 | 2.78                          | 0.30 | 0.22 | 1.12 | 15.7 |
| 2       | A       | 0–7                | 9.91          | 4.9 | 2.65                          | 0.44 | 0.06 | 0.94 | 47.9 |
|         | Bw1     | 7–38               | 4.17          | 4.8 | 0.32                          | 0.31 | 0.06 | 0.20 | 38.1 |
|         | Bw2     | 38–88              | 1.82          | 4.9 | 0.24                          | 0.28 | 0.07 | 0.18 | 28.2 |
|         | BC      | 88–109             | 0.53          | 4.9 | 0.58                          | 0.27 | 0.14 | 0.42 | 24.4 |
|         | C1      | 109–122            | 0.45          | 4.9 | 0.38                          | 0.19 | 0.15 | 0.33 | 22.6 |
|         | C2      | 122–146            | 0.15          | 5.3 | 0.30                          | 0.15 | 0.15 | 0.25 | 17.5 |
| 3       | A       | 0–28               | 3.73          | 5.0 | 0.37                          | 0.37 | 0.15 | 0.47 | 28.9 |
|         | Bt1     | 28–44              | 1.08          | 5.0 | 0.18                          | 0.32 | 0.13 | 0.32 | 17.6 |
|         | Bt2     | 44–68              | 0.59          | 5.1 | 0.21                          | 0.35 | 0.11 | 0.27 | 16.2 |
|         | Bt3     | 68–113             | 0.32          | 5.1 | 0.14                          | 0.15 | 0.11 | 0.27 | 15.2 |
|         | BCt1    | 113–200            | 0.27          | 4.9 | 0.14                          | 0.10 | 0.13 | 0.36 | 18.1 |
|         | A       | 0–28               | 3.02          | 5.0 | 1.15                          | 0.31 | 0.13 | 0.51 | 27.7 |
| 4       | Bw      | 28–42              | 1.72          | 4.8 | 0.21                          | 0.22 | 0.12 | 0.19 | 20.7 |
|         | Bt      | 42–75              | 0.90          | 5.1 | 0.23                          | 0.21 | 0.23 | 0.34 | 17.3 |
|         | 2Bt2    | 75–120             | 0.35          | 5.2 | 0.16                          | 0.25 | 0.19 | 0.38 | 15.3 |
|         | A       | 0–21               | 5.36          | 5.2 | 0.46                          | 0.33 | b.t  | 0.33 | 29.9 |
| 5       | Bw1     | 21–30              | 2.68          | 5.1 | 0.03                          | 0.21 | 0.02 | 0.33 | 23.1 |
|         | Bt1     | 50–100             | 0.74          | 5.2 |                               | 0.14 | 0.02 | 0.20 | 17.7 |
|         | Bt2     | 100–170            | 0.26          | 5.1 | 0.02                          | 0.19 | 0.02 | 0.12 | 16.9 |
|         | BCt1    | 170–200            | 0.19          | 4.7 | 0.03                          | 0.12 | 0.08 | 0.15 | 14.8 |
|         | AB      | 8–39               | 2.33          | 5.2 | 2.12                          | 0.20 | 0.14 | 0.61 | 21.3 |
| 6       | Bt1     | 39–92              | 0.97          | 5.3 | 2.04                          | 0.09 | 0.10 | 0.53 | 20.9 |
|         | Bt2     | 92–192             | 0.43          | 4.8 | 0.27                          | 0.12 | 0.10 | 0.39 | 17.4 |
|         | Bt3     | 192–232            | 0.32          | 5.1 | 0.14                          | 0.14 | 0.15 | 0.35 | 20.9 |
|         | Cr1     | 342–392            |               | 4.8 | 0.17                          | 0.17 | 0.18 | 0.39 | 21.4 |
|         | A       | 0–20               | 5.22          | 4.9 | 1.21                          | 0.32 | 0.11 | 0.48 | 33.9 |
| 7       | Bw      | 20–37              | 2.76          | 5.0 | 0.78                          | 0.25 | 0.22 | 0.40 | 27.2 |
|         | Bt      | 37–73              | 1.04          | 5.2 | 0.77                          | 0.09 | 0.08 | 0.85 | 14.0 |
|         | 2Bt1    | 73–140             | 0.56          | 4.9 | 0.10                          | 0.27 | 0.09 | 0.30 | 12.1 |
|         | 2Bt2    | 140–190            | 0.26          | 5.0 | 0.24                          | 0.10 | 0.09 | 0.16 | 15.2 |

Blanks indicate unanalyzed sample

b.t. indicates result of analysis was below detection

the decline occurs. In most terraces, the depth-dependent decline in  $A_{lo}$  and  $A_{lp}$  values occurs deeper and more gradually than the drop off in the  $Fe_o$  and  $Fe_p$ . The short-range order mineral concentration as interpreted from the  $A_{lo} + 0.5Fe_o$  value is

highest in A horizons and decreases with depth (Table 4; Fig. 5b). In the T2 soil, the oxalate and pyrophosphate extracts suggest possible andic or spodic soil materials (see below).  $A_{lo}$  and  $Fe_o$  values rapidly increase from T1 to a maximum in



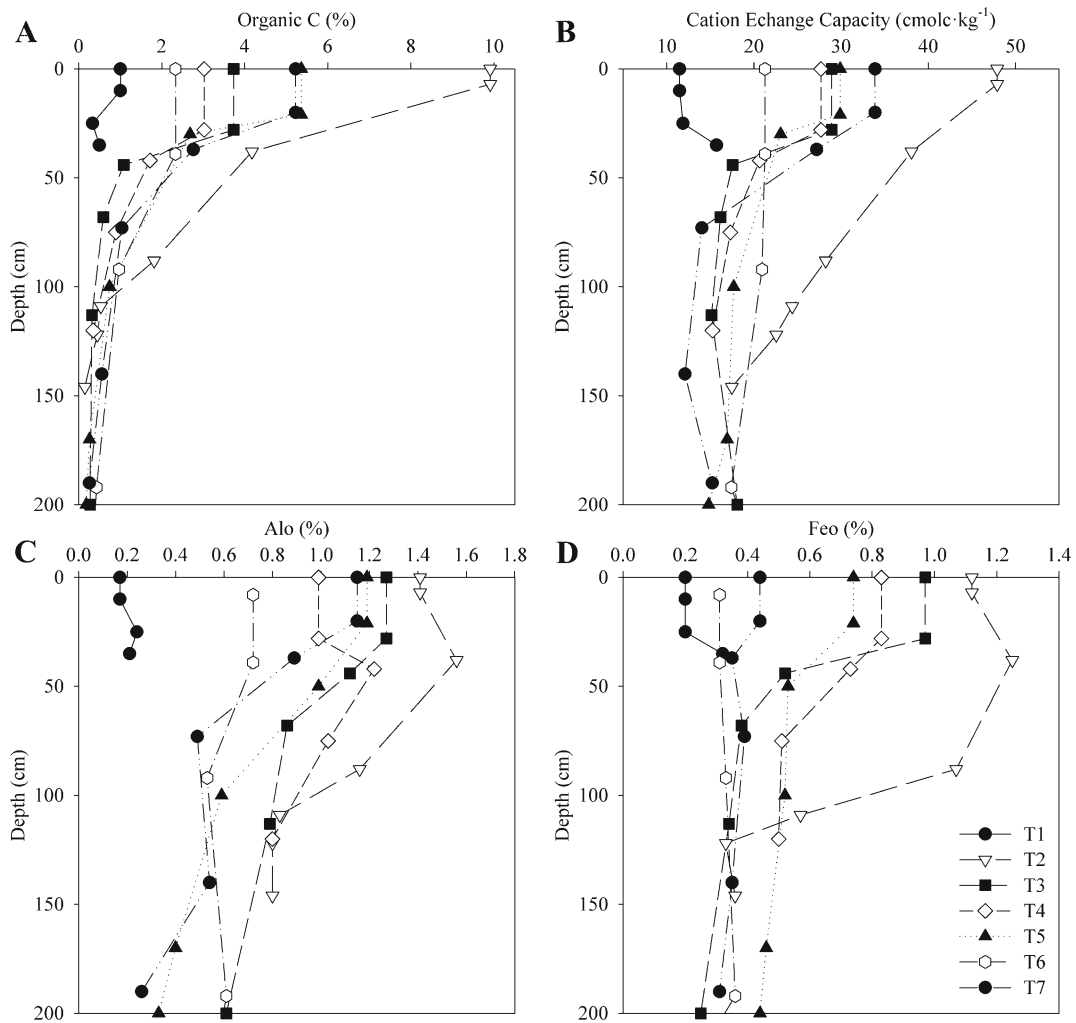


**Fig. 3** Depth distributions of organic C, cation exchange capacity, and extractable metals. Plots show upper and lower boundaries for horizons. For most terrace soils, contents of

organic C (a), CEC (b), organic and amorphous Al (c) and Fe (d) are highest near the surface and decline with depth

T2 and gradually decline with increasing terrace age and soil development (Fig. 2e).

Dithionite extractable Al (Ald) and Fe (Fed) are consistently low in the surface T1 soil (<0.4 % and <1.0 %, respectively) (Table 4). The first and third buried soils, however, display zones of small accumulations of extractable Al and Fe suggesting formation of cambic horizons. On all other terraces, soils have similar Ald amounts and depth trends such that Ald reaches a maximum (1.0–1.5 %) in the shallowest mineral horizon (A or AB) and declines with depth to 0.5–1.5 % in the B horizons. Fed shows strong depth-dependent trends within individual terraces

(Fig. 5c) and clear differences among them (Fig. 2a). Fed in all soils increases from A horizons to near-surface B horizons, and then declines with depth. Near-surface horizon Fed content and profile maxima values increase progressively from and 0.5–2.3 %, respectively, in the young terraces (T1 and T2), to 2.7–3.4 % and 3.2–4.2 % in the intermediate-aged terraces (T3 and T4), and then to 4.3–5.4 % and 6.0–7.3 % in the oldest terraces (T5, T6, and T7) (Fig. 5d).

The proportion of Fe in pedogenic form (Fed/Fet) increases with terrace age and contributes to the observed increase in soil redness and a decrease in RR values (Fig. 4a). All terraces except T1 and T2 have

**Table 4** Contents of extractable Al, Fe, and Si for selected horizons

| Terrace | Horizon | Pyrophosphate |         | Oxalate |         |         | Dithionite |         | Alo +<br>0.5Feo<br>(%) | Crystallinity<br>(1 - Feo/Fed) | Fed/Fet <sup>a</sup> | Al <sub>2</sub> O <sub>3</sub> /<br>SiO <sub>2</sub> |
|---------|---------|---------------|---------|---------|---------|---------|------------|---------|------------------------|--------------------------------|----------------------|--|
|         |         | Alp (%)       | Fep (%) | Alo (%) | Feo (%) | Sio (%) | Ald (%)    | Fed (%) |                        |                                |                      |  |
| 1       | A       | 0.10          | 0.05    | 0.17    | 0.20    | 0.29    | 0.10       | 0.49    | 0.28                   | 0.58                           | 0.24                 | 0.17   |
|         | C1      | 0.14          | 0.02    | 0.24    | 0.20    | 0.30    | 0.09       | 0.43    | 0.34                   | 0.55                           | 0.22                 | 0.17   |
|         | C2      | 0.10          | 0.05    | 0.21    | 0.32    | 0.80    | 0.18       | 0.53    | 0.37                   | 0.40                           | 0.25                 | 0.18   |
| 2       | A       | 1.18          | 0.61    | 1.41    | 1.12    | 3.13    | 1.45       | 2.26    | 1.97                   | 0.50                           | 0.61                 | 0.31   |
|         | Bw1     | 1.11          | 0.36    | 1.56    | 1.25    | 2.43    | 1.37       | 2.29    | 2.19                   | 0.45                           | 0.56                 | 0.35   |
|         | Bw2     | 0.59          | 0.16    | 1.16    | 1.07    | 2.10    | 1.05       | 2.34    | 1.69                   | 0.54                           | 0.56                 | 0.35   |
|         | BC      | 0.28          | 0.07    | 0.83    | 0.57    | 2.30    | 0.82       | 2.14    | 1.12                   | 0.73                           | 0.53                 | 0.32   |
|         | C1      | 0.32          | 0.03    | 0.80    | 0.33    | 2.54    | 0.59       | 0.88    | 0.96                   | 0.62                           | 0.31                 | 0.28   |
|         | C2      | 0.27          | 0.02    | 0.80    | 0.36    | 2.74    | 0.47       | 0.52    | 0.98                   | 0.31                           | 0.21                 | 0.25   |
| 3       | A       | 1.32          | 0.18    | 1.27    | 0.97    | 2.56    | 1.31       | 2.66    | 1.75                   | 0.64                           | 0.64                 | 0.31   |
|         | Bt1     | 1.11          | 0.05    | 1.12    | 0.52    | 2.96    | 1.21       | 2.91    | 1.37                   | 0.82                           | 0.68                 | 0.33   |
|         | Bt2     | 0.63          | 0.04    | 0.86    | 0.38    | 2.95    | 1.00       | 3.06    | 1.06                   | 0.87                           | 0.69                 | 0.35   |
|         | Bt3     | 0.30          | 0.04    | 0.79    | 0.34    | 1.09    | 0.84       | 3.19    | 0.96                   | 0.89                           | 0.74                 | 0.37   |
|         | BCt     | 0.32          | 0.05    | 0.61    | 0.25    | 2.65    | 0.69       | 2.50    | 0.73                   | 0.90                           | 0.68                 | 0.34   |
| 4       | A       | 0.91          | 0.23    | 0.99    | 0.83    | 1.85    | 1.19       | 3.36    | 1.41                   | 0.75                           | 0.71                 | 0.36   |
|         | Bw      | 0.48          | 0.09    | 1.22    | 0.73    | 2.78    | 1.14       | 3.33    | 1.58                   | 0.78                           | 0.65                 | 0.38   |
|         | Bt      | 0.38          | 0.03    | 1.03    | 0.51    | 2.68    | 1.07       | 3.61    | 1.29                   | 0.86                           | 0.71                 | 0.39   |
|         | 2Bt2    | 0.31          | 0.11    | 0.80    | 0.50    | 2.92    | 0.94       | 4.15    | 1.05                   | 0.88                           | 0.79                 | 0.38   |
| 5       | A       | 1.04          | 0.53    | 1.19    | 0.74    | 1.35    | 1.46       | 4.58    | 1.56                   | 0.84                           | 0.84                 | 0.41   |
|         | Bw      | 0.62          | 0.21    | 0.99    | 0.53    | 1.20    | 1.28       | 4.52    | 1.26                   | 0.88                           | 0.75                 | 0.45   |
|         | Bt1     | 0.53          | 0.07    | 0.59    | 0.52    | 1.40    | 1.09       | 6.02    | 0.85                   | 0.91                           | 0.90                 | 0.50   |
|         | Bt2     | 0.33          | 0.04    | 0.40    | 0.46    |         | 0.92       | 6.01    | 0.63                   | 0.92                           | 0.89                 | 0.56   |
|         | BCt1    | 0.05          | 0.04    | 0.33    | 0.44    |         | 0.68       | 4.78    | 0.55                   | 0.91                           | 0.82                 | 0.46   |
| 6       | AB      | 0.64          | 0.24    | 0.72    | 0.31    | 1.31    | 1.03       | 5.40    | 0.87                   | 0.94                           | 0.82                 | 0.79   |
|         | Bt1     | 0.49          | 0.09    | 0.53    | 0.33    | 0.49    | 0.97       | 7.34    | 0.69                   | 0.96                           | 1.00                 | 0.98   |
|         | Bt2     | 0.17          | 0.04    | 0.61    | 0.36    | 1.83    | 0.89       | 6.12    | 0.79                   | 0.94                           | 0.89                 | 0.72   |
|         | Bt3     | 0.29          | 0.02    | 0.55    | 0.19    |         | 0.58       | 3.61    | 0.64                   | 0.95                           | 0.62                 | 0.54   |
|         | CR1     | 0.23          | 0.02    | 0.29    | 0.11    | 0.49    | 0.46       | 3.15    | 0.35                   | 0.96                           | 0.76                 | 0.41   |
| 7       | A       | 0.75          | 0.28    | 1.15    | 0.44    | 1.33    | 1.19       | 4.34    | 1.37                   | 0.90                           | 0.76                 | 0.42   |
|         | Bw      | 0.53          | 0.19    | 0.89    | 0.35    | 1.70    | 1.12       | 5.65    | 1.07                   | 0.94                           | 0.94                 | 0.54   |
|         | Bt      | 0.35          | 0.18    | 0.49    | 0.39    | 1.26    | 0.91       | 6.75    | 0.69                   | 0.94                           | 0.88                 | 0.81   |
|         | 2Bt1    | 0.17          | 0.05    | 0.54    | 0.35    | 1.71    | 0.87       | 7.12    | 0.71                   | 0.95                           | 0.97                 | 0.70   |
|         | 2Bt2    | 0.12          | b.t     | 0.26    | 0.31    |         | 0.80       | 5.63    | 0.41                   | 0.95                           | 0.84                 | 0.68   |

Blanks indicate unanalyzed sample

b.t. indicates result of analysis was below detection

<sup>a</sup> Fed/Fet reflects the fraction of pedogenic to total Fe. Total Fe was converted from oxide into non-oxide form for use in this calculation

Fed/Fet values that increase with depth (Table 4), which reflects a higher degree of secondary forms of Fe in illuvial zones. Approximated here by 1 - Feo/Fed, the crystallinity of Fe-oxides decreases with depth (Table 4) and increases with terrace age (Fig. 4b). Other than in the youngest two terraces,

highest Al<sub>2</sub>O<sub>3</sub>/SiO<sub>2</sub> values occur in illuvial zones and likely reflect greater Si leaching and perhaps deposition of biogenic Si in surface horizons (Fig. 4b). Leaching of Si and accumulation of secondary Fe compounds occurs rapidly through the first 200 ky of soil development, but the rate subsequently slows

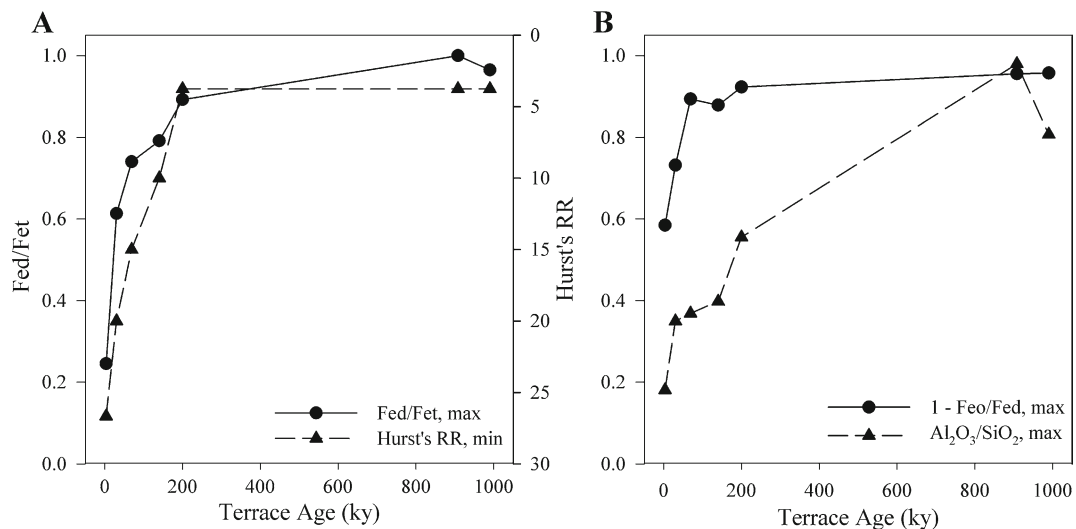


**Fig. 4** Age-trends related to forms and ratios of Fe, Al, and Si, crystallinity of iron oxides, and soil color. **a** Pedogenic to total Fe (Fed/Fet) and soil redness increase with increasing terrace

age, the latter reflected by a decrease in Hurst's Redness Rating. **b** Crystallinity and Al<sub>2</sub>O<sub>3</sub>/SiO<sub>2</sub> increase with increasing terrace age, the former reflected by an increase in 1 - Feo/Fed values

(Fig. 4a). Initially much of the pedogenic Fe is in short-range order mineral form (Feo), but after T2, crystallinity increases rapidly with terrace age as the iron compounds ripen into more stable phases (Fig. 4b).

## Discussion

### Soil development

The chronosequence properties suggest progressive pedogenesis that is dominated by transformation of primary minerals to secondary clays and metal oxyhydroxides. Time-dependent changes in soil properties include an increase in profile thickness, soil redness, and accumulation of secondary minerals. Quartz becomes enriched in the sand fraction at the expense of plagioclase and potassium feldspars. Pedogenic oxides of Al and Fe increase while non-quartz Si is either leached or locked up in secondary aluminosilicate clays. Clay content and expression of clay cutans increase with age. Pedogenic Fe comprises an increasing amount of total Fe, with an increasing degree of crystallinity. A striking feature of soil morphological evolution is reddening (Table 1; Fig. 4a) associated with a progressive increase in Fed/Fet, crystallinity (1 - Feo/Fed) and formation of iron-rich concretions. Short-range order aluminosilicate and iron minerals (extracted by oxalate) are well represented early but

decline as the crystalline clays and metal oxides (extracted by dithionite) accumulate. The T2 and T3 soils show the most rapid feldspar weathering, loss of exchangeable base cations, and the greatest accumulation of short-range order minerals.

The rates of changes in the soil properties indicate a change in dominant soil processes over the course of soil development. In the earliest stage, organic matter input and mineral weathering occur in weakly developed Entisols and Inceptisols. Short-range order metal oxide and aluminosilicate mineral contents rapidly increase to form Inceptisols with Andisol-like properties. With more time, continued weathering of primary minerals, ripening of metal oxides, and clay mineral synthesis lead to more strongly developed Ultisols. Base cation saturation and exchangeable Ca levels reach a minimum in the oldest sites, which suggest that nutrient cycling must become tighter to preserve the remaining cations.

### Soil classification

Based on *Soil Taxonomy* (Soil Survey Staff 2010), fluvial terrace soils change from Entisols (T1), to Inceptisols (T2) to Ultisols (T3 and older) (Table 5). The soils of T3–T7 are taxonomically distinguished by the presence and thickness of an argillic horizon, organic matter content, base cation saturation, and andic soil properties. The youngest soil of T1 lacks a B

**Table 5** Classification and selected properties relevant in taxonomy

| Terrace soil classification | Taxonomically relevant                        |                          |                                      |   |  |                                   |
|-----------------------------|---|--------------------------|--------------------------------------|---|--|-----------------------------------|
|                             | Humult Organic C in 1 m (kg·m <sup>-2</sup> ) | Palehumult Max. Clay (%) | Depth <sup>d</sup> of Max. Clay (cm) | Depth that clay drops below “Max. Clay - 20 %” (cm) | Clay in depth of “Max. Clay - 20 %”(%) | Clay in 1 m (kg·m <sup>-2</sup> ) |
| 1 Typic Udipsamment         | 9.0 <sup>e</sup>                              | 4.5 <sup>f</sup>         | 0 <sup>f</sup>                       |   |  |                                   |
| 2 Andic Dystustept          | 26.3  | 34.5                     | 88                                   | *   | *                                      | 295.0                             |
| 3 Andic Haplohumult         | 15.6  | 44.1                     | 68                                   | 200   | 16.6                                   | 437.2                             |
| 4 Andic Palehumult          | 15.1  | 43.9                     | 75                                   | >290  | 26.5                                   | 447.3                             |
| 5 Andic Palehumult          | 21.7  | 56.1                     | 50                                   | 400   | 10.1                                   | 537.9                             |
| 6 Typic Palehumult          | 15.6 <sup>a</sup>                             | 74.5                     | 39                                   | 192   | 47.6                                   | 731.7 <sup>b</sup>                |
| 7 Andic Palehumult          | 18.4  | 67.8                     | 37                                   | 270   | 41.3                                   | 608.0 <sup>c</sup>                |

Soil classification is based on *Keys to Soil Taxonomy* (Soil Survey Staff 2010). Taxonomically relevant data presented here were used for soil classification of the terrace soils into suborders and great groups: high amounts of C is reflected by the *Hum* suborder; the *And* subgroup indicates high levels of Alo and Feo and low soil bulk density; *Pale* great group designates an extensive zone of clay accumulation in which the depth of maximum clay is >1 m above the depth where clay content drops at least 20 % of maximum value  
\*Lithogenic contact occurs at base of solum; percent clay does not drop to <20 % of the profile-maximum

<sup>a</sup> Due to absence of data for T6 6–8 cm, the 8 cm thickness was added to the underlying horizon thickness; thus the presented value is likely an underestimation of the organic C in 1 m

<sup>b</sup> The same method was used for the Clay in 1 m calculation in order to account for the absence of 0–8 cm data; thus, the presented value is likely an overestimation of the clay content in 1 m

<sup>c</sup> Bulk density was not available for the deepest horizon within the 1 m; the bulk density of the overlying horizon was used in its place

<sup>d</sup> Depth corresponds to upper horizon boundary

<sup>e</sup> Includes organic C from a buried soil

<sup>f</sup> Though T1 was analytically studied to a depth of ~1.8 m, for this comparison, only the youngest soil corresponding to 0–35/40 cm in T1 was considered

horizon, is coarse textured, shows minimal signs of pedogenic development, and is an Entisol. The second and fourth buried soil on T1 have cambic horizons, which suggests that Inceptisols can form in <3.5 ky (Almond et al. 2007).

The T2 soil is an Inceptisol even though the upper 40 cm resembles andic material because of its high concentrations of oxalate extractable sesquioxides (Table 4), low bulk density (Table 2), and high organic carbon content (Table 3). However, the soil is not dark enough for recognition as andic material and lacks a high enough percent base saturation required for designation as a melanic epipedon. The upper 40 cm in the T2 soil also resembles spodic material but misses the color criterion. Furthermore, there is no overlying zone of eluviation typical of Spodosols. It is likely that the oxalate extractable metals correspond not to allophane or imogolite as would be the case in Andisols and Spodosols (Soil Survey Staff 1999), but to metal-humus compounds because Sio is low, and both

Alp/Alo and Fep/Feo are >0.5 (Table 4). Below the andic- and spodic-like zone, there is a sufficient clay increase for an argillic horizon (38–109 cm) but no evidence (such as the presence of clay cutans) that the clay was illuviated.

The soils on T3 and older terraces classify in the Humult suborder and contain argillic horizons with low base saturation and high amounts of carbon (>9 kg·m<sup>-2</sup> in the upper 1 m; Table 5). Alfisols are not recognized anywhere in the sequence because base saturation decreases to below 35 % in the soil on T2 and remains low thereafter; before argillic horizons develop in soils on T3 and older terraces. The soils on T4 and older terraces have deep, thick zones of clay accumulation and classify as Palehumults. On surfaces other than T1 and T6, soils have in the upper 75 cm low bulk density and elevated levels of Alo and Alp which allow placement into the Andic subgroup. The exclusion of T6 from the Andic subgroup may reflect erosion of the upper part of its solum.

## Soil genesis on fluvial terraces and coastal terraces

Bockheim et al. (1992, 1996) formulated a pedogenic model for the udic soil moisture regime (MAP of 1,900 mm) and isomesic soil temperature regime (MAAT 10 °C) region of coastal Oregon based on marine terrace chronosequences. Those soils formed in surficial deposits of sand derived from in-situ and reworked beach sediments. Some but not all marine terraces have thin caps of eolian silt likely dating from the latest Pleistocene or early Holocene. Vegetation is predominately Sitka spruce on the younger marine terraces and Douglas fir and Western hemlock on the older terraces.

In Bockheim et al.'s (1996) coastal terrace model of soil formation, andisolization and podzolization dominate early stages of pedogenesis (~10–105 ky) and lead to the development of nascent spodic properties in Inceptisols, which then develop into Spodosols. During an intermediate stage (~105–200 ky), spodic processes are supplanted by clay neof ormation and lessivage which drive formation of Ultisols. Progressive clay accumulation leads to more strongly expressed Ultisols (see Fig. 3 in Bockheim et al. 1996). This conceptual model also accounts for soil variability within individual terraces of comparable ages, namely by site-specific drainage conditions (Bockheim et al. 1992; Bockheim et al. 1996; Langley-Turnbaugh and Bockheim 1997, 1998). For example, soils on intermediate and old terraces had spodic character in poorly drained or somewhat poorly drained conditions but fit the criteria for Ultisols in well-drained locations.

Our fluvial terrace chronosequence has ustic/xeric soil moisture regime, mesic (but not isomesic) soil temperature regime, coarse-textured, arkosic parent material, and is dominated by Douglas fir forest (Almond et al. 2007). Soil genesis fits some aspects of the Bockheim model of pedogenesis. Comparisons of age-trends and specific properties of the fluvial and coastal terrace chronosequences reveal the following: (1) Both chronosequences exhibit increasing degrees of weathering with increasing terrace age, ultimately leading to an endpoint expression of Ultisols. The chronosequences differ, however, in the rate of weathering and extent of expression of weathering-related features. (2) During the initial stages of soil formation, soils of both chronosequences have andic-like properties, but the sites subtly differ in the depth of occurrence and extent of expression of

andic-like properties. (3) Spodosols are present in coastal young and intermediate sites, but they are absent in the inland fluvial terrace chronosequence.

Both chronosequences display systematic changes in pedogenic properties leading to deep profiles and thick zones of clay accumulation. In the coastal terrace chronosequence, Bockheim et al. (1996) reported an increase in total profile and profile-maximum concentrations of Fed and clay, a decrease in feldspars relative to quartz in the fine sand fraction, and increases in solum thickness and thickness of clay-enriched zones. Furthermore, they noted similar rates of pedogenic development as those reported in previous studies of marine terraces in California (Muhs 1982; Merritts et al. 1991). The fluvial terrace chronosequence also displays these age-trends, although the absolute amounts of accumulated Fed and clay are larger and the accumulation processes occur faster relative to the coastal terrace sequences (Fig. 5). The argillic horizons of the Ultisols are expressed to varying degrees within the coastal and fluvial terrace soils. Whereas Bockheim et al. (1996) reported a systematic increase in depth to maximum clay content with marine terrace age, the opposite age-trend occurs in our fluvial terrace chronosequence (Table 5). Although Fed increases with terrace age in both coastal and fluvial settings, Fed maximum percentages and mass to 1 m are greater in fluvial sites. In the coastal sites the near-surface eluvial zones are depleted in Fed, which contrasts with the fluvial chronosequence, in which Fed accumulates in the surface horizons and throughout the profile with little evidence for strong eluviation. Residual enrichment, rather than translocation, is likely the main driver for iron accumulation in the fluvial terraces.

Andisol-like properties are observed in young soils in the coastal chronosequence—specifically, the Typic Haplorthods of Cape Blanco Terrace (site 89–39) and Whisky Run Terrace (site 89–48) of Bockheim (1992, 1996)—and T2 of the fluvial terrace chronosequence, which is classified as an Andic Dystrustept. The andic properties in the young soils resemble other Andisols and Andisol-like soils previously described in non-volcanic settings in the Pacific Northwest, which have low  $S_{io}$  levels (<0.5 %) and high  $Alp/Al_o$  values (>0.5) with oxalate extractable fractions dominated by metal-humic complexes (Baham and Simonson 1985; Nettleton et al. 1982). However, these soils do not classify as Andisols. In the case of T2, the relevant horizons are not dark enough (value and chroma are

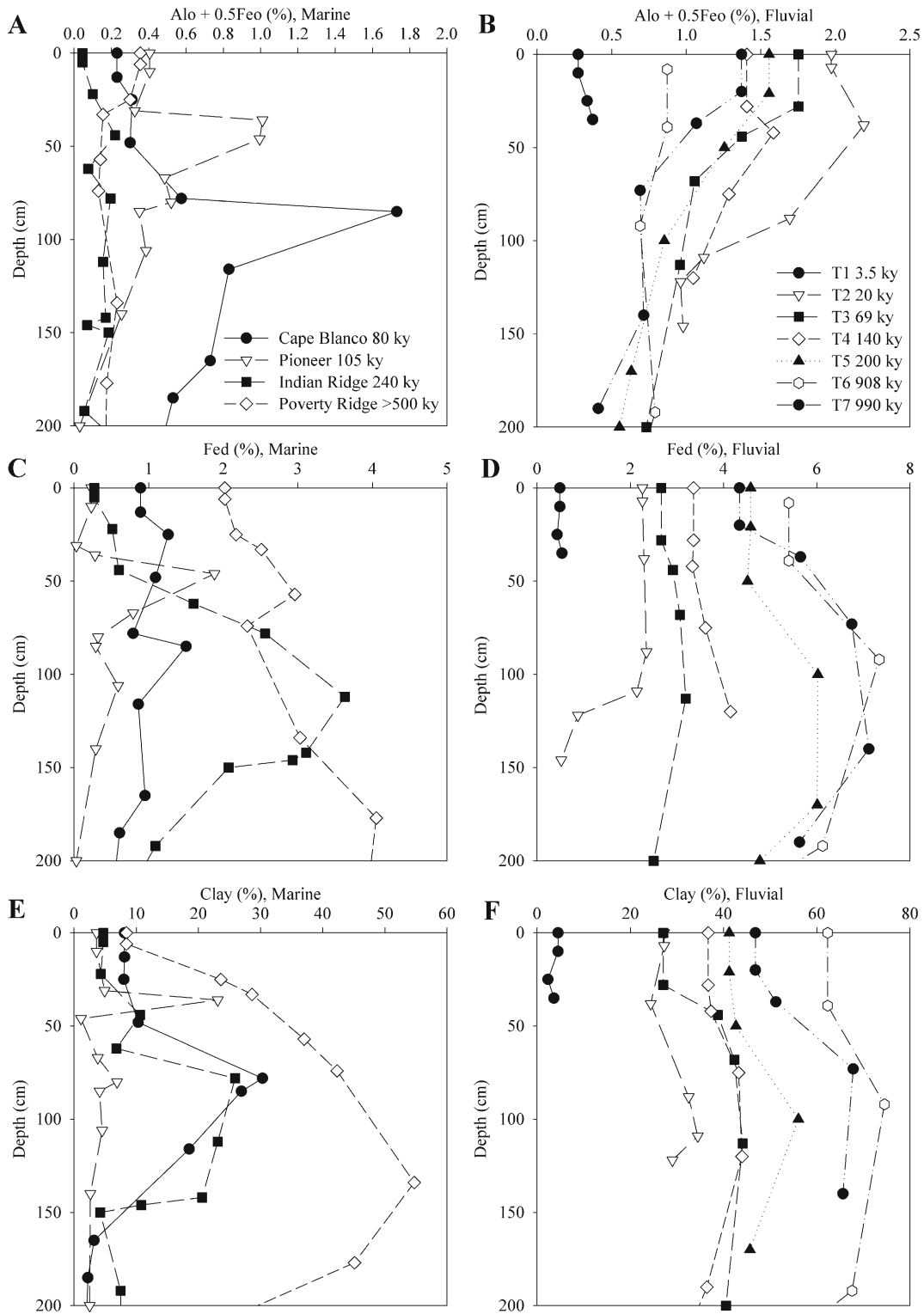


**Fig. 5** Depth distributions for various measures in the marine and fluvial terrace chronosequences. For most marine terrace soils, profile-maxima of Alo + 0.5Feo (a), Fed (c), and clay (e)

occur in a subsoil horizon. Fluvial terrace soils also have sub-surface zones of profile-maxima Fed (c) and clay (f), but show surface maxima in Alo + 0.5Feo (b) contents

3). In the coastal terrace soils, concentrations of oxalate extractable metals in the shallowest horizons are too low.

The young coastal soils classify as Spodosols. Concentrations of oxalate-extractable metals are lowest in eluvial surface horizons and a maximum in illuvial subsurface horizons. Fluvial terrace soils, by contrast, have elevated concentrations of oxalate-extractable metals in surface A and shallow subsurface B horizons (Fig. 3c,d; Table 4). It is possible that the persistence of near-surface andic characteristics and formation of metal-organic complexes in the fluvial terrace chronosequence is driven by organic matter quality and rate of decomposition.

Although there are other differences between the coastal and fluvial chronosequences, it is the absence of Spodosols that most strongly challenges inland extrapolation of the coastal soil genesis model described by Bockheim et al. (1996). It is difficult to evaluate causality of this absence of Spodosols in the fluvial terrace chronosequence, given that the coastal and fluvial sites have similar soil forming factors, and multiple possible pathways of Spodosol formation (Lundström et al. 2000). Podsolization requires a mechanism (for instance, acidity, fluctuating redox conditions, or low molecular weight organic ligands) to first mobilize metals in the near surface and to then transport them downwards. There must also be a mechanism to arrest mobile compounds in the subsoil (for instance, changes in pH, metal-organic saturation, or contrasts in pore size). Mobilization and arresting mechanisms operate differently in differing pedogenic environments, making it difficult to generalize about or compare processes operating in coastal or inland environments with certainty. However, there are several possible explanations for the prevalence of podzolization along the Pacific coast and its absence in the inland mountains: differences in climate, vegetation, and parent material, each of which are evaluated below.

Environmental factors that could produce differences in soil formation

Spodosol formation is favored in cool moist climates where precipitation is greater than evapotranspiration (Lundström et al. 2000). Since the Oregon coast and Coast Range receive between 1,500 and 2,500 mm of rain annually there should be adequate moisture for

Spodosol genesis. The variation in rainfall is controlled partly by compression of oceanic air masses as they reach land (Elliott and Reed 1973; Trump and Elliott 1976) and by air mass cooling due to orographic rise over the Coast Range (Smith et al. 2005). The complexity of air mass – land interaction makes it difficult to predict rainfall amounts in sparsely instrumented terrain. It is probable that more rain falls in the Oregon Coast Range, particularly at higher elevations, than in the coastal study area of Bockheim et al. (1996). Thus, if more rain drives a greater tendency toward Spodosol formation, the inland Coast Range might be expected to host them. Differences in temperature could also be important in differentiating processes of soil formation. Subtly cooler temperatures have been associated with stronger expression of spodic properties in Michigan (Schaeztl 1996) and Pennsylvania (Stanley and Ciolkosz 1981). During the relatively dry summer months, the marine terraces are often enveloped by low clouds and fog, which keeps air temperatures low and maintains soil moisture. Compared with the marine terrace soils, inland fluvial terrace soils experience higher contrasts in summer-winter air temperatures higher summer temperatures, and a higher likelihood of soil drying during the summer months. Drying in turn can lead to more rapid ripening of metastable short-range order minerals (extracted by oxalate) into crystalline aluminosilicate clays and Fe and Al oxyhydroxides and perhaps less easily mobilized metals. Thus, the relatively subtle seasonal difference in water balance between the coast and Coast Range could differentiate processes into translocation of mass in the former and in situ immobilization in the latter.

Spodosol formation is favored by vegetation that produces low molecular weight organic acids during decomposition (Lundström et al. 2000; Mossin et al. 2001) that provide ligands to mobilize metals. Sitka spruce, the dominant tree species in the coastal sites of Bockheim et al. (1996), produces strong organic acids and is known to acidify soils following land cover transformation (Nielson et al. 1999; Nørnberg et al. 1993). Douglas fir, prevalent inland in the fluvial terrace sites, produces slightly less acidic litter (McCull 1973; Reich et al. 2005; Mueller et al. 2012; Hobbie et al. 2007) hence the organic anions are often less important than bicarbonate (Van Miegroet and Cole 1985), suggesting a somewhat higher pH in soils with Douglas fir than in soils with

Sitka spruce. Douglas fir accumulates and cycles higher levels of calcium compared with Sitka spruce (Turner 1981; Reich et al. 2005) which can ameliorate acidity and provide a chemical flocculant to minimize eluviation. Despite these differences in chemistry, Douglas fir has been implicated in podzolization (Lundström et al. 2000). Western hemlock also produces considerable amounts of organic acids (Finzi et al. 1998). The presence of Sitka spruce and Western hemlock on the coastal terraces favors the lower pH observed in near surface horizons, metal eluviation, and formation of spodic materials. The coastal setting is subject to inputs of marine aerosol, which can enhance podzolization because  $\text{Na}^+$  can flood cation exchange complexes and displace Al and its hydroxy compounds (Nørnberg et al. 1993), and  $\text{Cl}^-$  can take the place of organic acids as a counter anion during leaching processes (Bockheim and Langley-Turnbaugh 1997). Some of the coastal Spodosols occur under Douglas fir and Western hemlock, suggesting that vegetation alone does not control formation of spodic properties (Bockheim et al. 1992). On the fluvial terraces where Douglas fir dominates, surface soil horizons have higher pH which is less conducive to organic ligand mobilization, and the soil profiles show no evidence for eluviation of metals.

Formation of Spodosols is favored by soil fabric with a coarse skeleton, which maintains large pores and relatively low surface area from which surface sorbed metals can be stripped by chelating molecules (Lundström et al. 2000). Sandy soils provide these conditions whereas clay-rich soils do not. The large surface area provided by clay tends to sorb the low molecular weight organic acids which minimizes potential colloidal redistribution (Masiello et al. 2004) and contributes to soil reddening (Duchaufour and Souchier 1978). The greywacke that is ground into the parent material in both settings provide quartz and weatherable minerals, and there is little difference in sand mineralogy between coastal and fluvial sites. In both cases it is possible that sand derived from greywacke could be composed of considerable amounts of clays, such as magnesium chlorite, that would be released quickly during weathering processes (Merritts et al. 1991; Chadwick et al. 1990). There is a strong similarity in the particle size distribution (texture was loamy sand or sand in coastal Cu horizons; same with fluvial T1 unweathered sediments) and in mineralogy (Quartz/Feldspars of C horizons)

for coastal and inland soils, which suggests that parent material alone cannot account for differences in soil evolution between the two chronosequences. Thus, the more rapid increase in clays in the fluvial terrace chronosequence is likely due to different rates of weathering and mineral transformations. Clay synthesis and transformation can be strongly enhanced by wetting and drying processes (Ziegler et al. 2003; Chadwick and Chorover 2001; Chadwick et al. 2003). It is possible that a difference in water balance is being expressed as metal chelation and clay losses/translocation out of the profiles in the more consistently moist coastal area and as clay production and stabilization/accumulation in the interior of the Coast Range. However, eventual development of Ultisols means that clay synthesis is the long-term result in both areas. It appears that variation in climate and vegetation may result in differences in pedogenic processes on short time scales but may not affect the end product.

Differences in dust input to the chronosequences could be important in determining pathways of pedogenesis (Simonson 1995; Eger et al. 2012). The majority of the coastal terraces in the Pacific Northwest and specifically, SW Oregon, are capped with loess that have thicknesses ranging from 20 to 70 cm (Langley-Turnbaugh and Bockheim 1997, 1998; Bockheim et al. 1992; Bockheim et al. 1996). The silty loess is superimposed on a sand-rich parent material, and overlies portions of even the oldest terraces (Nettleton et al. 1982). The resulting pore-size discontinuity can promote mobilization of metals during periods of soil saturation and low redox potential above the discontinuity, and deposition of spodic materials below (Bockheim et al. 1992). The contact with material below can be abrupt and is particularly striking on intermediate and older terraces where there is an argillic horizon below the loess cap (Bockheim et al. 1992; Nettleton et al. 1982). Markewich and Pavich (1991) interpreted similar bisequal and multisequal soils in the Southeastern US as having originated in two distinct parent materials—namely, the upper sequum with spodic properties formed in eolian sediments, and a lower sequum with an older argillic horizon formed in the underlying sediment. Similarly, Nettleton et al. (1982) suggested that the Spodosols on the older Oregon coastal terraces were loess-dependent not age-dependent features. It is likely that more work needs to be done to evaluate the relative



pedogenic roles of underlying parent material transformation and eolian inputs in the coastal setting.

## Conclusions

There are several likely reasons why Spodosols form preferentially along the coast and are not favored in more inland locations. The cooler, overcast coastal summers contribute to less seasonal drying and support Sitka spruce forests that produce copious amounts of low molecular weight organic acids that can drive metal chelation. Near the coast, sea salt input affects the nature of cation and anion leaching, which in turn changes soil solution chemistry and formation of spodic materials. In contrast to the coast, inland summers are warmer and drier, conditions which might favor more rapid mineral ripening. The seasonally dry inland soils support Douglas fir, which cycles Ca more tightly than spruce and produces less organic acids, producing an environment less conducive to Spodosol formation. The role of minor differences in climate and differences in vegetation are intertwined and with the existing data it is not possible to be certain if one or both drive the observed differences. Perhaps a more important difference is that the coastal settings are near a substantial beach source of dust, which may provide different chemical and physical environments that enhance podzolization. Particle size data suggest that there is minor dust input to the fluvial terrace soils as well, but not enough to develop the distinct stratigraphic layers seen on the coast. It is likely that podzolization is a dominant process in young terraces on the coast because weathering has not released enough clay to shut down cheluviation. In the fluvial terraces, the T2 soil fills a similar age and development niche but the metals (and their associated organic matter) precipitate in the surface horizons and have andic rather than spodic properties. In each case there has not yet been enough weathering and clay formation to drive the soil to Ultisol status. We conclude that there are fundamental differences in the environmental conditions between the coast and interior, which drives differences in early pedogenic pathways but which lead to the same end product. The differences between the coastal and mountainous environments are subtle but profound with respect to pedogenic models.

**Acknowledgments** Funding for this project was supplied in part by the Geomorphology and Land Use Dynamics program,

Division of Earth Sciences, National Science Foundation (EAR-0952186). We are grateful to two anonymous reviewers, one of whom provided very detailed suggestions on how to improve the manuscript.

## References

- Almond P, Roering JJ, Hales TC (2007) Using soil residence time to delineate spatial and temporal patterns of transient landscape response. *J Geophys Res* 112 (F03S17):doi:10.1029/2006JF000568. doi:10.1029/2006JF000568
- Baham J, Simonson GH (1985) Classification of soils with andic properties from the Oregon coast. *Soil Sci Soc Am J* 49:777–780
- Barrett LR, Schaetzl RJ (1992) An examination of podzolization near Lake Michigan using chronofunctions. *Can J Soil Sci* 72:527–541
- Barrett LR, Schaetzl RJ (1993) Soil development and spatial variability on geomorphic surfaces of different age. *Phys Geogr* 14:39–55
- Bierman P, Clapp E, Nichols K, Gillespie A, Caffee M (2001) Using cosmogenic nuclide measurements in sediments to understand background rates of erosion and sediment transport. *Landscape erosion and evolution modeling*. Kluwer Academic Plenum, New York
- Birkeland PW (1999) *Soils and geomorphology*, 3rd edn. Oxford University Press, New York
- Bockheim JG (1980) Solution and use of chronosequence in studying soil development. *Geoderma* 24:71–85
- Bockheim JG, Langley-Turnbaugh S (1997) Biogeochemical cycling in coniferous ecosystems on different aged marine terraces in coastal Oregon. *J Environ Qual* 26:292–301
- Bockheim JG, Kelsey HM, Marshall JM III (1992) Soil development, relative dating, and correlation of late Quaternary marine terraces in southwestern Oregon. *Quat Res* 37:60–74
- Bockheim JG, Marshall JG, Kelsey HM (1996) Soil-forming processes and rates on uplifted marine terraces in southwestern Oregon, USA. *Geoderma* 73:39–62
- Bull WB (1991) *Geomorphic responses to climate change*. Oxford University Press, New York, NY
- Chadwick OA, Chorover J (2001) The chemistry of pedogenic thresholds. *Geoderma* 100(3–4):321–353
- Chadwick OA, Brimhall GH, Hendricks DM (1990) From a black to a gray box - a mass balance interpretation of pedogenesis. *Geomorphology* 3:369–390
- Chadwick OA, Gavenda RT, Kelly EF, Ziegler K, Olson CG, Elliott WC, Hendricks DM (2003) The impact of climate on the biogeochemical functioning of volcanic soils. *Chem Geol* 202:195–223
- Duchaufour PH, Souchier B (1978) Roles of iron and clay in genesis of acid soils under a humid, temperate climate. *Geoderma* 20:15–26
- Eger A, Almond PC, Condron LM (2012) Upbuilding pedogenesis under active loess deposition in a super-humid, temperate climate - quantification of deposition rates, soil

- chemistry and pedogenic thresholds. *Geoderma* 189–190:491–501
- Elliott WP, Reed PK (1973) Oceanic rainfall off the Pacific Northwest Coast. *J Geophys Res Oceans* 78:941–948
- Finzi AC, Van Breemen N, Canham CD (1998) Canopy tree - soil interactions within temperate forests: species effects on pH and cations. *Ecol Appl* 8(2):440–446
- Heimsath AM, Dietrich WE, Nishiizumi K, Finkel R (2001) Stochastic processes of soil production and transport; erosion rates, topographic variation and cosmogenic nuclides in the Oregon Coast Range. *Earth Surf Process Landf* 26(5):531–552
- Heller PL, Dickinson K (1985) Submarine ramp facies model for delta-fed, sand-rich turbidite systems. *AAPG Bull* 69(6):960–976
- Heller PL, Peterman ZE, O'Neil JR, Shafiqullah M (1985) Isotopic provenance of sandstones from the eocene tye formation, Oregon Coast Range. *Geol Soc Am Bull* 96:770–780
- Hobbie SE, Ogdahl M, Chorover J, Chadwick OA, Oleksyn J, Zytowski R, Reich PB (2007) Tree species effects on soil organic matter dynamics: the role of soil cation composition. *Ecosystems* 10:999–1018. doi:10.1007/s10021-007-9073-4
- Hurst VJ (1977) Visual estimation of iron in saprolite. *Geol Soc Am Bull* 88(2):174–176
- Jackson ML (1954) Soil chemical analysis: advanced course. Parallel Press, Madison
- Jenny H, Arkley RJ, Schultz AM (1969) The Pygmy forest-Podsol ecosystem and its dune associates of the Mendocino Coast. *Madrono* 20:60–74
- Kelsey HM (1990) Late Quaternary deformation of marine terraces on the Cascadia Subduction Zone near Cape Blanco, Oregon. *Tectonics* 9:983–1014
- Kelsey HM, Ticknor RL, Bockheim JG, Mitchell CE (1996) Quaternary upper plate deformation in coastal Oregon. *Geol Soc Am Bull* 108(7):843–860
- Langley-Turnbaugh SJ, Bockheim JG (1997) Time-dependent changes in pedogenic processes on marine terraces in Coastal Oregon. *Soil Sci Soc Am J* 61:1428–1440
- Langley-Turnbaugh SJ, Bockheim JG (1998) Mass balance of soil evolution on late Quaternary marine terraces in Coastal Oregon. *Geoderma* 84:265–288
- Lundström US, Van Breemen N, Bain D (2000) The podsolization process. A review. *Geoderma* 94(2–4):91–107
- Markewich HW, Pavich MJ (1991) Soil chronosequence studies in temperate to subtropical, low-latitude, low-relief terrain with data from the eastern United States. *Geoderma* 51(1–4):213–239
- Masiello CA, Chadwick OA, Southon J, Torn MS, Harden JW (2004) Weathering controls on mechanisms of carbon storage in grassland soils. *Global Biogeochem Cycles* 18(4):4023.4021–4023.4029
- McCull JG (1973) Environmental factors influencing ion transport in a Douglas-fir forest soil in western Washington. *J Ecol* 61(No. 1):71–83
- McFadden LD, Knuepfer PLK (1990) Soil geomorphology: the linkage of pedology and surficial processes. *Geomorphology* 3(3/4):197–205
- McKeague JA (1967) An evaluation of 0.1 M Pyrophosphate and pyrophosphate-dithionite in comparison with oxalate as extractants of the accumulation products in podzols and some other soils. *Can J Soil Sci* 47:97–99
- McKeague JA, Day JK (1966) Dithionite- and oxalate-extractable Fe and Al as aids in differentiating various classes of soils. *Can J Soil Sci* 46:13–22
- Mehra OP, Jackson ML (1960) Iron oxide removal from soils and clays by a dithionite-citrate system buffered with sodium bicarbonate. *Clays Clay Miner* 7:317–327
- Merritts DJ, Chadwick OA, Hendricks DM (1991) Rates and processes of soil evolution on uplifted marine terraces, northern California. *Geoderma* 51(1–4):241–275
- Milne JDG, Clayden B, Singleton PL, Wilson AD (1995) Soil description handbook. Manaaki Whenua Press, Lincoln, New Zealand
- Montgomery DR (2001) Slope distributions, threshold hillslopes, and steady-state topography. *Am J Sci* 301(4–5):432–454
- Moore DM, Reynolds RC (1997) X-ray diffraction and the identification of clay minerals, 2nd edn. Oxford University Press, New York
- Mossin L, Jensen BT, Nørnberg P (2001) Altered podzolization resulting from replacing heather with Sitka spruce. *Soil Sci Soc Am J* 65:1455–1462
- Mueller KE, Eissenstat DM, Hobbie SE, Oleksyn J, Jagodzinski AM, Reich PB, Chadwick OA, Chorover J (2012) Tree species effects on coupled cycles of carbon, nitrogen, and acidity in mineral soils at a common garden experiment. *Biogeochemistry*. doi:10.1007/s10533-011-9695-7
- Muhs DR (1982) A soil chronosequence on Quaternary marine terraces, San Clemente Island, California. *Geoderma* 28:257–283
- Nettleton WD, Parsons RB, Ness AO, Gelderman FW (1982) Spodosols along the southwest Oregon coast. *Soil Sci Soc Am J* 46:593–598
- Nielson KE, Ladekar UL, Nørnberg P (1999) Dynamic soil processes on heathland due to changes in vegetation in oak and Sitka Spruce. *For Ecol Manage* 114:107–116
- Nørnberg P, Sloth L, Nielson KE (1993) Rapid changes in sandy soils caused by vegetation changes. *Can J Soil Sci* 73:459–468
- NRCS (2003) Soil moisture regimes map. National Resources Conservation Services. <http://soils.usda.gov/use/world-soils/mapindex/smr.html>. Accessed 05/12/2012
- Orr EL, Orr WN, Baldwin EM (1992) *Geology of Oregon*. Kendall/Hunt, Dubuque
- Patching WR (1987) Soil Survey of Lane County Area, Oregon. United States Department of Agriculture, Soil Conservation Service, Washington, D.C.
- Reich PB, Oleksyn J, Modrzyński J, Mrozinski P, Hobbie SE, Eissenstat DM, Chorover J, Chadwick OA, Hale B, Tjoelker MG (2005) Linking litter calcium, earthworms and soil properties: a common garden test with 14 tree species. *Ecol Lett* 8:811–818. doi:10.1111/j.1461-0248.2005.00779.x
- Reneau SL, Dietrich WE (1991) Erosion rates in the Southern Oregon Coast Range: evidence for an equilibrium between hillslope erosion and sediment yield. *Earth Surf Process Landf* 16(4):307–322
- Roering JJ, Kirchner JW, Dietrich WE (1999) Evidence for nonlinear diffusive sediment transport on hillslopes and

- implications for landscape morphology. *Water Resour Res* 35(3):853–870
- Ryu I-C (2003) Petrography, diagenesis and provenance of Eocene Tyee Basin sandstones, southern Oregon Coast Range: new view from sequence stratigraphy. *The Island Arc* 12(398–410)
- Schaetzl RJ (1996) Spodosol-Alfisol intergrades: Bisequal soils in NE Michigan, USA. *Geoderma* 74:23–47
- Schaetzl RJ, Barrett LR, Winklyer JA (1994) Choosing models for soil chronofunctions and fitting them to data. *Eur J Soil Sci* 45:219–232
- Simonson RW (1995) Airborne dust and its significance to soils. *Geoderma* 65:1–43
- Singer MJ, Fine P, Verosub KL, Chadwick OA (1992) Time dependence of magnetic susceptibility of soil chronosequences on the California coast. *Quat Res* 37:323–332
- Smith RB, Barstad I, Bonneau L (2005) Orographic precipitation and Oregon's climate transition. *J Atmos Sci* 62:177–191
- Snavelly P, Wagner H, MacLeod N (1964) Rhythmic-bedded eugeosynclinal deposits of the tyee formation, Oregon Coast Range. In: Merriam DF (ed) Symposium on cyclic sedimentation, December 1964. Kansas Geological Survey, p 636
- Soil Survey Staff (1999) Soil taxonomy: a system of soil classification for making and interpreting soil surveys (2nd Ed.), Soil Survey Investigations Report No. 436. vol Agriculture Handbook. National Resource Conservation Service, USDA
- Soil Survey Staff (2010) Keys to soil taxonomy. 11 edn. Natural Resources Conservation Service, USDA
- Stanley SR, Ciolkosz EJ (1981) Classification and genesis of Spodosols in the central Appalachians. *Soil Sci Soc Am J* 45:912–917
- Trump CL, Elliott WP (1976) Fine-scale variations of rainfall in Western Oregon. *Water Resour Res* 12:556–560
- Turner J (1981) Nutrient cycling in an age sequence of western Washington Douglas-fir stands. *Ann Bot* 48(2):159–169
- Van Miegroet H, Cole DW (1985) Acidification sources in red alder and Douglas fir soils – Importance of nitrification. *Soil Sci Soc Am J* 49:1274–1279
- Ziegler K, Hsieh JCC, Chadwick OA, Kelly EF, Hendricks DM, Savin SM (2003) Halloysite as a kinetically controlled end product of arid-zone basalt weathering. *Chem Geol* 202:461–478